Somnath Ghosh
Christopher Woodward
Craig Przybyla *Editors*

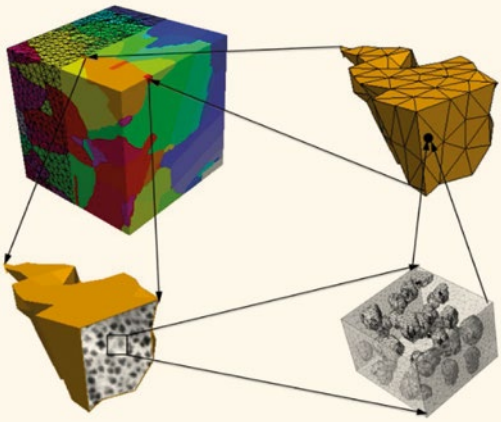

Integrated Computational Materials Engineering (ICME)

Advancing Computational and Experimental Methods

Springer

Integrated Computational Materials Engineering (ICME)

Somnath Ghosh • Christopher Woodward
Craig Przybyla
Editors

Integrated Computational Materials Engineering (ICME)

Advancing Computational and Experimental Methods

Springer

Editors
Somnath Ghosh
Departments of Civil, Mechanical Engineering and Materials Science & Engineering
Johns Hopkins University
Baltimore, MD, USA

Craig Przybyla
Air Force Research Laboratory/RX
Wright-Patterson Air Force Base
Dayton, OH, USA

Christopher Woodward
Air Force Research Laboratory/RX
Wright-Patterson Air Force Base
Dayton, OH, USA

ISBN 978-3-030-40561-8 ISBN 978-3-030-40562-5 (eBook)
https://doi.org/10.1007/978-3-030-40562-5

This book is dedicated to all researchers in the Center of Excellence on Integrated Materials Modeling (CEIMM) and Air Force Research Laboratories, whose dedication made this possible.

Preface

The Integrated Computational Materials Engineering (ICME) thrust is an integral part of the Materials Genome Initiative (MGI) that has been launched to advance multi-scale materials modeling for addressing complex materials structure-property-performance-processing relationships. It is viewed as the integration of computational tools for materials discovery, design, and sustained development, with information technologies, component design systems, and manufacturing process simulations, to foster improved product performance, manufacturability, and sustainability. The ICME thrust is aimed at novel innovations in fundamental science and engineering of materials for providing significant tools that can bridge the gap between materials engineering and component design. Robust theoretical, computational, and experimental methods pertaining to materials, performances, and process models are emerging as a consequence of this thrust. High-performance structural applications that have been hitherto restricted to available structural materials with limited ability to integrate new materials into the design process are now opening up to new possibilities with the advances made in this thrust.

While structural engineering has greatly benefited from the introduction of effective computational tools, such as finite element, finite difference, and boundary element methods, advances in computational and experimental methods have been more piecemeal for the materials community. This is due to the underlying complexities in processing-structure-property relationships for different classes of materials like metals, polymer matrix composites, and ceramics. The materials science paradigm for structural materials relates the internal structure, produced through processing, to the desired properties and response. The ICME approach has helped create synergistic advances in materials research, blending advanced computational mechanics with materials characterization, multi-scale modeling, and experimental property acquisition, providing a strong computational backbone for integrating computational tools and data handling methods with high pedigree experimental methods for accelerating materials transition into component design to achieve improved product manufacturability, performance, and sustainability.

In the spirit of fostering foundational advances in computational and experimental methodologies supporting the ICME theme, the Materials and Manufacturing Directorate of the Air Force Research Laboratory at Wright Patterson Air Force Base and the Air Force Office of Scientific Research jointly initiated the *Center of Excellence on Integrated Materials Modeling (CEIMM)* in 2012, with Johns Hopkins University as the lead institution. Other major partners were the University of California at Santa Barbara and the University of Illinois at Urbana-Champaign. CEIMM was focused on the development of fundamental science and common threads of computational and experimental methods pertaining to structural materials. The central philosophy was to overcome limitations of empiricism-based phenomenological models through physics-based 4-D spatiotemporal multi-scaling approaches, transcending materials classes and boundaries between computational materials science and computational mechanics. Research in CEIMM has developed novel theoretical, computational, and experimental methods for advancing the state of the art in science and engineering of ICME-related fields without being material-specific. This includes mechanical modeling of high-temperature metals and composite materials including predicting spatial and temporal response and properties like strength, crystal plasticity, fracture, and fatigue. Significant advances have been made in computational multi-scale modeling, materials characterization, and experiments to efficiently describe the evolution of heterogeneities and outlier structures and their effect on the balance of structural properties. A suite of methods and models have been developed for two classes of structural materials, namely, nickel-based superalloys and epoxy-matrix carbon fiber composites. The unifying platform is accomplished through the incorporation of fundamental physics-based multi-spatial and temporal scale modeling, in lieu of conventional empiricism.

This book discusses significant research advancements in ICME that have taken place under the aegis of CEIMM. It includes contributions from other thought leaders in the field, who are leading researchers in ICME from prominent academic institutions and government laboratories. It also introduces theoretical, computational, and experimental methods, advancing the state of the art in science and engineering of the ICME fields for structural materials. A special focus is on two structural materials listed below:

1. *Ni-based superalloys*, e.g., René 88DT, characterized by polycrystalline microstructures with sub-grain heterogeneities in the form of secondary $\gamma - \gamma'$ phases;
2. *Polymer matrix composites* with carbon fibers in epoxy matrix.

Four themes are broadly addressed in this book. They are:

- *Multi-scale Data Acquisition, Characterization, and Image-Based Virtual Models:* This introduces methods of acquiring high-fidelity materials microstructural data and methods of advanced microstructural characterization and addresses the generation of three-dimensional statistically equivalent virtual models.

- *Physics-Based Multi-scale Model Development:* The development of image-based micromechanical computational models with morphological and crystallographic details is discussed. The models represent dominant deformation and failure mechanisms at each scale. Comprehensive methods of identifying representative volume elements (RVEs) based on microstructure and materials response or properties are detailed. Associated boundary conditions for RVEs with non-uniform microstructures are derived. Hierarchical multi-scale models for connecting mechanisms at different scales are discussed. Spatial scales encompass atomistic scales, mesoscales of coarse-grained models and discrete dislocations, and microscales of polyphase and polycrystalline microstructures.
- *Experimental Methods for Constitutive Models and Failure Processes:* Novel experiments for aiding the development of computational models, with information on mechanisms and data for calibration and validation are addressed. Experiments characterize relevant properties and microstructural responses over a range of operating conditions.
- *Probabilistic Modeling and Uncertainty Quantification:* This discusses probabilistic models accounting for stochastic distributions of materials microstructure and properties.

The relations between microstructural morphology, crystallography, and mechanisms to the materials response at different scales are investigated.

This book is a collection of 14 chapters that discuss aspects of ICME developments, ranging from physics-based multi-scale computational methods to experimental data acquisition and uncertainty quantification. The first eight chapters deal with experiments and modeling of polycrystalline alloys, with a focus on Ni-based superalloys. Chapter 1 details methods of 3D microstructural data acquisition for predicting monotonic and cyclic properties of superalloys. It provides information on the distribution of important structural features, namely, precipitates, annealing twins and grains. Data structures and workflow tools for generating and analyzing materials data in an ICME context are discussed in Chap. 2. Chapter 3 details fundamental aspects of statistically equivalent virtual microstructures and microstructure and property-based statistically equivalent representative volume elements (M-SERVE and P-SERVE) of Ni-based superalloys at multiple scales. The two specific scales considered are the sub-grain scale of intragranular $\gamma - \gamma'$ microstructures and the polycrystalline scale of grain ensembles with annealing twins. Chapter 4 provides an overview of micro-tensile experiments and characterizations for the superalloy René 88DT. A computational micromechanics model of the polycrystalline superalloys application to Inconel 718 is presented in Chap. 5. A combination of simulations and tests, together with computational homogenization strategies, is used to predict the mechanical behavior of these superalloys. A comparison of deterministic and non-deterministic calibration methods for crystal plasticity model parameters is made in Chap. 6. Chapter 7 reports on the soft-coupled linkage between a macroscale damage model and mesoscale calculations of a suite of polycrystal instantiations of tantalum. A macroscale model is used to represent a

tantalum on tantalum plate impact experiment and predict the point in time in the loading profile when porosity is likely to initiate. Chapter 8, the last chapter in the category, projects a framework for quantifying effects of characterization error on the predicted local elastic response in polycrystalline materials.

Chapter 9 presents a unique materials agnostic data-driven framework to develop structure-property linkages and addresses curation of materials' knowledge from the available data sets in computationally efficient manner to extract and use the processing-structure-property relationships. Chapters 10 through 13 focus on the development of ICME-related techniques for polymer matrix composites. Chapter 10 provides a review of multi-scale modeling efforts involving molecular dynamics modeling of epoxy and epoxy-based composites for structural, thermal, mechanical, and interfacial properties. In Chap. 11, a novel microstructural statistics-informed boundary condition has been developed for statistically equivalent representative volume elements (serve) of polydispersed elastic composites. Chapters 12 and 13 relate to transverse failure of unidirectional composites, including sensitivity to interfacial properties and geometric modeling. Chapter 14, the final chapter, deals with the challenges in modeling dynamic behavior of granular media, reactive powder mixtures, energetic and composite materials, and multiphase materials. It discusses possible ways of exploring topology, property contrasts, and microstructural morphology to link dynamic response to micro- and mesoscale behavior.

It is our expectation that this book will address many of the current gaps in the ICME theme and will be a leading resource for practitioners of ICME. The materials presented in this book will enable researchers in academia, government laboratories, and industries to comprehend and approach ICME-related issues involved in predicting materials performance and failure with a focus on the structure-materials interaction. The book is expected to be an important scientific compilation of high value to the ICME community, especially in mechanical engineering, materials science and engineering, aerospace engineering, civil engineering, and other disciplines. We gratefully acknowledge the research support from the Air Force Office of Scientific Research (Program Managers Drs. Fariba Fahroo and Ali Sayir) and the Air Force Research Laboratories (Chief Scientists Dr. Barry Farmer and Timothy J. Bunning). This work would not have been possible without the financial and technical support of Johns Hopkins University and the Air Force Research Laboratory's Materials and Manufacturing Directorate. Chris Woodward recognizes the insightful discussions with Dr. Jeff Bauer during the conceptual phases of the center and the significant contributions and guidance of Dr. Tim Breitzman during the first 2 years of the project.

We, the editors, would like to extend our sincere thanks and appreciation to all the contributing authors of this volume for embracing our vision and providing excellent state-of-the-art articles on different topics in the general field. We are also thankful to the Springer editorial staff for their support with the production of this book. Somnath Ghosh expresses his love and deep appreciation to his wife, Chandreyee, for her constant encouragement and support throughout this project.

Craig Przybyla expresses his love and appreciation to his wife, Laura, and children, Elizabeth, Dallin, William, Christian, Emma, and Jane, for their unfailing support and encouragement in all his professional endeavors. Chris Woodward recognizes the love and support of his wife, Leslie, over the course of this project.

Baltimore, MD, USA — Somnath Ghosh
Dayton, OH, USA — Craig Przybyla
Dayton, OH, USA — Christopher Woodward
September 2019

Acknowledgment

This work has been supported through Grant No. FA9550-12-1-445 to the Center of Excellence on Integrated Materials Modeling (CEIMM) at Johns Hopkins University awarded by the AFOSR/RSL Computational Mathematics Program (Program Managers Dr. Fariba Fahroo and Dr. Ali Sayir). This support is gratefully acknowledged.

Contents

Contributors

Angel Agrawal Department of Aerospace Engineering, University of Illinois, Urbana, IL, USA

Akbar Bagri Departments of Mechanical and Civil Engineering, Johns Hopkins University, Baltimore, MD, USA

Geoffrey Bomarito Durability, Damage Tolerance and Reliability Branch, NASA Langley Research Center, Hampton, VA, USA

David Brandyberry Department of Aerospace Engineering, University of Illinois, Urbana, IL, USA

C. A. Bronkhorst Theoretical Division, Los Alamos National Laboratory, Los Alamos, NM, USA
Department of Engineering Physics, University of Wisconsin, Madison, WI, USA

H. Cho School of Mechanical and Aerospace Engineering, Korea Advanced Institute of Science and Technology, Daejeon, Republic of Korea

Amanda Criner Materials and Manufacturing Directorate, Air Force Research Laboratory, Dayton, OH, USA

Aitor Cruzado Department of Aerospace Engineering, Texas A&M University, College Station, TX, USA
Center for Intelligent Multifunctional Materials and Structures, TEES, Texas A& M University, College Station, TX, USA

Sean P. Donegan Air Force Research Laboratory, Materials and Manufacturing Directorate, Wright-Patterson Air Force Base, Dayton, OH, USA

David W. Eastman Department of Mechanical Engineering, Johns Hopkins University, Baltimore, MD, USA

Mclean P. Echlin The Materials Department, University of California Santa Barbara, Santa Barbara, CA, USA

Jaafar A. El-Awady Department of Mechanical Engineering, Whiting School of Engineering, The Johns Hopkins University, Baltimore, MD, USA

Philippe Geubelle Department of Aerospace Engineering, University of Illinois, Urbana, IL, USA

Somnath Ghosh Departments of Civil, Mechanical Engineering and Materials Science & Engineering, Johns Hopkins University, Baltimore, MD, USA

Manny Gonzales Materials and Manufacturing Directorate, Air Force Research Laboratory, WPAFB, Dayton, OH, USA

Lori Graham-Brady Department of Civil Engineering, Johns Hopkins University, Baltimore, MD, USA

G. T. Gray III Materials Science and Technology Division, Los Alamos National Laboratory, Los Alamos, NM, USA

Michael A. Groeber Air Force Research Laboratory, Materials and Manufacturing Directorate, Wright-Patterson Air Force Base, Dayton, OH, USA
The Ohio State University, Department of Integrated Systems Engineering, Columbus, OH, USA

Kevin J. Hemker Department of Mechanical Engineering, Johns Hopkins University, Baltimore, MD, USA

Jacob Hochhalter Department of Mechanical Engineering, University of Utah, Salt Lake City, UT, USA

George Jefferson Air Force Research Laboratory/RX, Wright-Patterson Air Force Base, Dayton, OH, USA

Anthony Klepacki Department of Aerospace Engineering, University of Illinois, Urbana, IL, USA

Dhirendra V. Kubair Department of Civil Engineering, Johns Hopkins University, Baltimore, MD, USA

William C. Lenthe The Materials Department, University of California Santa Barbara, Santa Barbara, CA, USA

Patrick Leser Durability, Damage Tolerance and Reliability Branch, NASA Langley Research Center, Hampton, VA, USA

William Leser Durability, Damage Tolerance and Reliability Branch, NASA Langley Research Center, Hampton, VA, USA

V. Livescu Materials Science and Technology Division, Los Alamos National Laboratory, Los Alamos, NM, USA

Javier Llorca IMDEA Materials Institute, Getafe, Madrid, Spain
Department of Materials Science, Polytechnic University of Madrid, Madrid, Spain

P. W. Marcy Computer, Computational, and Statistical Sciences Division, Los Alamos National Laboratory, Los Alamos, NM, USA

Christopher Montgomery Department of Materials Science and Engineering, University of Illinois, Urbana, IL, USA

Ahmad Najafi Department of Mechanical Engineering and Mechanics, Drexel University, Philadelphia, PA, USA

Kyle Nixon Department of Aerospace Engineering, University of Illinois, Urbana, IL, USA

Triplicane Parthasarathy UES, Inc, Dayton, OH, USA

Dipen Patel UES, Inc, Dayton, OH, USA

Maxwell Pinz Departments of Mechanical and Civil Engineering, Johns Hopkins University, Baltimore, MD, USA

Tresa M. Pollock The Materials Department, University of California Santa Barbara, Santa Barbara, CA, USA

Craig Przybyla Air Force Research Laboratory/RX, Wright-Patterson Air Force Base, Dayton, OH, USA

Michael Rossol Department of Materials Science and Engineering, University of Illinois, Urbana, IL, USA

Tim Ruggles Durability, Damage Tolerance and Reliability Branch, National Institute of Aerospace, Hampton, VA, USA

Javier Segurado IMDEA Materials Institute, Getafe, Madrid, Spain
Department of Materials Science, Polytechnic University of Madrid, Madrid, Spain

Paul A. Shade Materials and Manufacturing Directorate, Air Force Research Laboratory, Wright-Patterson AFB, Dayton, OH, USA

Maryam Shakiba Department of Civil and Environmental Engineering, Virginia Tech., Blacksburg, VA, USA

Nancy Sottos Department of Materials Science and Engineering, University of Illinois, Urbana, IL, USA

Jean-Charles Stinville The Materials Department, University of California Santa Barbara, Santa Barbara, CA, USA

Naresh N. Thadhani School of Materials Science and Engineering, Georgia Institute of Technology, Atlanta, GA, USA

Michael D. Uchic Materials and Manufacturing Directorate, Air Force Research Laboratory, Wright-Patterson AFB, Dayton, OH, USA

S. A. Vander Wiel Computer, Computational, and Statistical Sciences Division, Los Alamos National Laboratory, Los Alamos, NM, USA

Noah Wade Department of Civil Engineering, Johns Hopkins University, Baltimore, MD, USA

James Warner Durability, Damage Tolerance and Reliability Branch, NASA Langley Research Center, Hampton, VA, USA

George Weber Departments of Mechanical and Civil Engineering, Johns Hopkins University, Baltimore, MD, USA

Christopher Woodward Air Force Research Laboratory/RX, Wright-Patterson Air Force Base, Dayton, OH, USA

Xiawa Wu Department of Mechanical Engineering, Whiting School of Engineering, The Johns Hopkins University, Baltimore, MD, USA
Mechanical Engineering, The Pennsylvania State University, The Behrend College, Erie, PA, USA

Saikumar Yeratapally Durability, Damage Tolerance and Reliability Branch, National Institute of Aerospace, Hampton, VA, USA

Scott Zacek Department of Aerospace Engineering, University of Illinois, Urbana, IL, USA

Xiang Zhang Department of Mechanical Engineering, University of Wyoming, Laramie, WY, USA

The original version of this book was revised: A new co-author has been added in Chapter 12. The correction to this book is available at https://doi.org/10.1007/978-3-030-40562-5_15

Acquisition of 3D Data for Prediction of Monotonic and Cyclic Properties of Superalloys

McLean P. Echlin, William C. Lenthe, Jean-Charles Stinville, and Tresa M. Pollock

1 Superalloys and Fatigue

Turbine engines have continuously improved in performance and efficiency due to advances in materials and coatings, combined with the application of advanced thermomechanical, heat transfer, and aerodynamic design methodologies. Turbine disks are among the most safety-critical components in an aircraft engine and have therefore been the subject of extensive development and characterization studies [1–3]. Polycrystalline nickel-base superalloys are the typical material of choice for turbine disks due to their high fatigue resistance and ultimate tensile strength and good thermomechanical and thermochemical stability at elevated temperatures [4, 5]. Powder metallurgy processing is used to produce disk components with highly controlled grain size distributions, controlled inclusion (carbide and nitride) content via powder stock filtering, and near net shape part geometries [1–5]. Inclusion content and grain structure have both been shown to be influential in the fatigue life of disk alloys [6, 7]. An improved predictive capability of the mechanical performance of these alloys is required to enhance life prediction and reliability as well as guide the development of new alloys and processing paths.

Predicting fatigue properties of superalloys is particularly challenging, due to the localized character of the plasticity during cycling and its strong dependence on material structure. The schematic in Fig. 1 shows the microstructure of a polycrystalline superalloy, containing annealing twins as well as the $L1_2$ γ' precipitate strengthening phase, and the approximate length scales at which they

M. P. Echlin (✉) · W. C. Lenthe · J.-C. Stinville · T. M. Pollock
The Materials Department, University of California Santa Barbara, Santa Barbara, CA, USA
e-mail: mechlin@ucsb.edu; jeancharles_stinville@ucsb.edu; tresap@ucsb.edu

S. Ghosh et al. (eds.), *Integrated Computational Materials Engineering (ICME)*,
https://doi.org/10.1007/978-3-030-40562-5_1

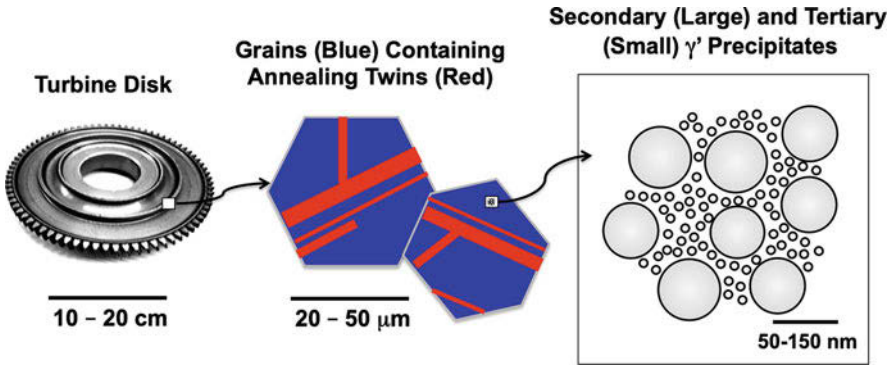

Fig. 1 Turbine disks (left) are often made from supersolvus nickel superalloys, such as René 88DT. This class of polycrystalline superalloys used for disks have microstructure at various length scales from precipitate structure (10's–100's nm as shown on the right) to twin related domain structure (10's–100 μm as shown in the center) with grains containing multiple, fine twinned structures of varying sizes that are crystallographically related to the parent material. They are strengthened by $L1_2$ γ' precipitates, which can exist over a range of length scales, depending on the processing conditions. Populations of secondary and tertiary γ' particles exist within the γ matrix phase (right), with the secondary particles typically being around 100 nm in diameter in René 88DT

exist. The fraction of $\Sigma 3$ annealing twin boundaries, a product of the processing path, can approach 46% by 2D measurement [8] or 70% by 3D measurement of the total boundary length fraction [9]. There is relatively limited crystallographic texture in these materials as a result of powder metallurgy processing or forging under nominally superplastic conditions. Depending on the alloy composition and processing route, populations of secondary and tertiary γ' particles exist within the γ matrix phase. The γ' precipitates inhibit the passage of dislocations through the γ matrix [5, 10], by requiring them to either shear through or bow around the ordered precipitates or cross-slip to continue to glide, effectively strengthening the material up to the solvus temperature of the precipitates. Typically, powder metallurgy consolidated components are oil quenched from near 1150 °C and then aged at 760 °C to produce a volume fraction near 40% of secondary and tertiary γ' precipitates [3].

In powder metallurgy superalloys such as René 88DT [1–3] cracks initiate in large grains that are in the tail of the size distribution and contain favorably oriented annealing twin boundaries [8, 11, 12] or at nonmetallic inclusions [7, 13, 14]. Though the annealing twin boundaries form during thermomechanical processing, the mechanisms by which they form are still not understood well enough to fully control their size and distribution. The relatively small grain size combined with moderate levels of $L1_2$ ordered precipitates imparts yield strengths above 1 GPa [4]. The relatively small grain size also limits the maximum length over which strain localization and slip events can occur over [6, 15, 16], before impinging on the adjacent high angle grain boundary, causing dislocation pileups.

Fatigue cracks typically initiate at the "weakest link" of the material structure. Rigorous models for fatigue thus require knowledge of the volume of the material that must be interrogated to capture the "rare" combinations of material structure that result in early strain localization and subsequent crack initiation [6, 7]. This, in turn, requires three-dimensional information on the distribution of important structural features: precipitates, annealing twins, grains, and in some cases carbides, nitrides, and oxides.

Nickel-base superalloys used for disks have microstructure at various length scales from precipitate structure (10's–100's nm) to twin related domain structure (10's–100 μm) with grains containing multiple, fine twinned structures of varying sizes that are crystallographically related to the parent material.

2 Importance of 3D Data

Many materials can be characterized using targeted 2D sections to analyze the microstructure, especially when the microstructure is isotropic and its features can be captured with well-known distributions [17, 18]. However, 2D inferences about structure and crystallography will be incomplete when investigating materials with rare features or heterogeneously distributed microstructure [17, 19, 20].

Nickel-base superalloys used for disks have microstructure at various length scales from precipitate structure (10's–100's nm) to twin related domain structure (10's–100 μm) with grains containing multiple, fine twinned structures of varying sizes that are crystallographically related to the parent material. Full 3D characterization is required to quantify the geometrical characteristics of the twins as well as to capture the five grain boundary parameters (three orientation parameters and two boundary normal parameters) [21–23]. The twin structures, which have been shown to be critical for the localization of strain [15, 16] and eventually the initiation of fatigue cracks [8, 11, 12], can be thin compared to the grain structure (μm thick) and may or may not extend across the entire grain.

A range of 3D tomography techniques have emerged in recent years that utilize femtosecond pulsed lasers [24, 25], mechanical polishing [26–29], broad ion beams [30], focused ion beams (FIB) [31–33], plasma FIBs [21, 34], and microtomes or serial block face SEM imaging [35, 36] to remove material in a serial sectioning approach. If only grain information is needed, then a combination of near-field [37–39] and far-field X-ray imaging allows for direct, nondestructive 3D characterization [40–44]. With current data collection and reconstruction methods, the X-ray diffraction methods have difficulty reconstructing crystallographic features that are below 5–10 μm in size, including fine twin structure, and also with crystals with preexisting strain gradients such as in samples that have been plastically deformed. Here we focus on serial sectioning approaches, due to the presence of thin micron-scaled annealing twins which are challenging to characterize with X-ray techniques.

Manual serial sectioning polishing techniques are effective for relatively coarse sectioning resolutions, especially if fiducial depth markers are incorporated; how-

ever much more advanced robotic polishing systems have been developed for optical imaging [45] and electron microscopy [26–29]. Currently, cm^3 volumes have been captured using the AFRL/RoboMet LEROY sectioning systems, as well as entire turbine blade components [46] using manual polishing approaches. For SEM imaging combined with robotic serial sectioning, the vacuum cycling and sample transfer time sets a limit on the minimum cycle time, which makes experiments with limited SEM imaging more time-consuming compared to other electron-optics-based serial sectioning systems.

FIB and Xe-plasma FIBs (PFIB) are rather limited with respect to the total accessible volume that can be analyzed as well as the types of material and speed at which materials can be sectioned. Microtomes have been shown to be useful, but primarily for biological samples and soft structural materials such as aluminum and polymers, and microanalytical analysis is challenging due to the extreme mechanical deformation imparted at the cut face.

X-rays have proven difficult to access large volumes of material with μm-scale microstructural features, although the techniques for software reconstruction are rapidly improving allowing access to deformed metallic samples [47, 48] and in situ dislocation imaging [49]. The advantages of X-ray diffraction contrast tomography (DCT) and the TriBeam femtosecond laser-based technique can be found elsewhere [50]. The resolution of synchrotron DCT and the high energy diffraction microscopy (HEDM) have dramatically improved [47], especially due to new reconstruction algorithms that identify grains and diffraction spots. These codes are actively being improved by the growing community of DCT users and scientists, facilitated by the open repositories at the beamlines and the open-sourced nature of the code. Routine access to synchrotron facilities can be challenging and requires careful preparation, motivating efforts for the development of a range of lab-based X-ray techniques that can be made available more broadly and with short notice. The available lab-scaled DCT systems [51, 52] are most effective for in situ experiments on materials with coarser grains than those accessible by synchrotron X-ray diffraction experiments and mostly for undeformed samples; however the reconstruction codes and scanning speeds are improving rapidly.

3 The TriBeam

The TriBeam microscope, shown in Fig. 2, is a modified FEI/Thermo Fisher Scientific Versa 3D focused ion beam scanning electron microscope (FIB-SEM) designed for high-speed, low-damage, bulk (mm^3-scaled) serial sectioning [24, 25]. A femtosecond laser beam has been incorporated into the FIB-SEM chamber with scanning lens, optics, and an alignment system. Multimodal data may be collected between material removal steps using a range of detectors for grain orientation information (electron backscatter diffraction – EBSD), chemical information (energy dispersive X-ray spectroscopy – EDS), atomic density (backscatter electron detector), and topographical and morphological information (secondary electron

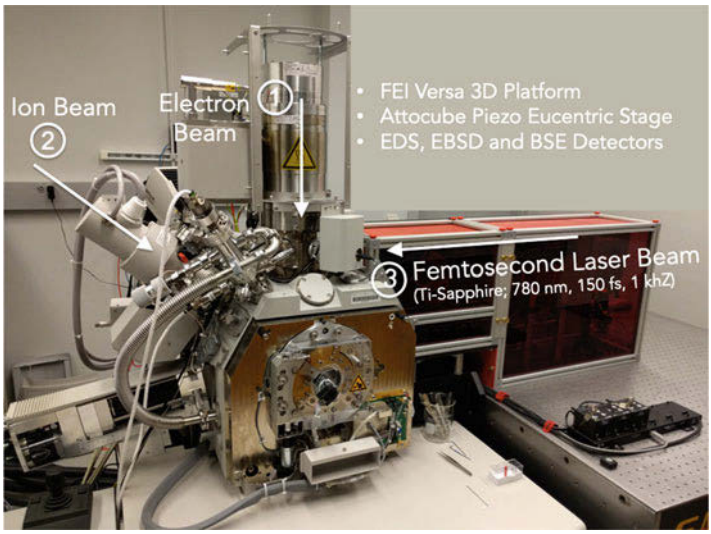

Fig. 2 The TriBeam microscope. The optics and beamline is contained within the red box on the right. The electron and focused ion beam are indicated. The femtosecond laser and beamline are directly aligned into the FIB-SEM via a coupled floating optics table

detector). Previous studies have shown that the damage resulting from femtosecond laser ablation is limited to dislocation injection in structural materials [53, 54]. To date, a wide range of materials including metals [55–57], ceramics [50], composites [58], and semiconductors [59] have been imaged in 3D using the TriBeam. The stock mechanically driven microscope stages are used to position the sample into the scanned laser beam (down to 0.5–1 μm slice thickness), or custom attocube piezoelectric stages can be utilized for slice thicknesses below 1 μm. However, the reliability and stiffness of the stock microscope stages are superior.

A typical 3D nickel dataset contains several hundred slices, with each slice requiring 1–100 min for acquisition, depending on the imaging modalities, imaging resolution, and whether FIB cleanup is required. The femtosecond laser ablation material removal step (1–3 min) is a very small fraction of the total slice time, which is typically dominated by the resolution at which EBSD data is gathered and whether FIB cleanup is performed.

The data in Table 1 shows the slice times that would be required for a hypothetical collection of a 1 mm^3 volume TriBeam dataset, with and without FIB cleanup and with 1 μm cubic voxels. Ga+ FIB cleaning requires approximately 1 min per every 20,000 μm^2 at glancing angles between 3 and 10°. The time required for cleanup does not change with glancing angle because the FIB dosage per area is held constant, resulting in increased dwell times at more glancing FIB beam angles. Experiments that do not require a FIB cleanup step reduce the total cycle time significantly, as shown in the last column in Table 1. Materials that do not require FIB cleanup in order to obtain acceptable quality EBSD patterns generally

Table 1 Times and percent of total cycle time required for imaging steps, material removal, stage moves, and surface cleanup that would be required during a 1 mm^3 experiment with 1 μm cubic voxel resolution

Operation	Slice time (min)	% of total cycle time	% of total cycle time (no FIB)
EBSD	30	33.7	76.9
Glancing FIB	50	56.1	-
SEM imaging	3	3.4	7.7
Fs laser Abl.	3	3.4	7.7
Stage moves	3	3.4	7.7

have good thermo-mechanical properties [53, 54]. Furthermore, new TriBeam instruments [60] that are based on a Xe-plasma FIB (PFIB) platform can perform focused ion beam cleanup with 30 kV and μA's of current, reducing the cleanup time by at least a factor of 20×. However, PFIB ion columns are still 3–4 orders of magnitude slower in terms of material removal speeds than a femtosecond laser, affirming the need for a multibeam system. The EBSD collection times described can easily scale to be much longer if the mapping resolution in x and y is finer than 1μm over a 1 mm^2 mapping area.

The latest CMOS-based EBSD cameras can collect patterns at rates up to 3000–5000 points per second. These cameras attain high pattern collection speeds through binning modes, whereby the full resolution of the camera is reduced by averaging the intensity from square regions of pixels. Binning increases the electron collection per binned pixel area and therefore allows for the reduction in exposure times, increasing pattern collection speed. Furthermore, the binned pattern resolutions are reduced, expediting the transfer rates between the hardware and decreasing computational times for indexing. These very high speeds are useful for gathering information suitable for grain mapping of single phase materials that diffract well, using Hough-based EBSD pattern indexing [61, 62]. In practice, larger EBSD pattern sizes are required for gathering more detailed information than grain maps while using Hough indexing, such as subgrain misorientation gradients, multiple phase indexing, and overlapping pattern information near grain boundaries. In this case, a longer exposure time and lower binning modes are necessary (slower collection speeds) for enhanced EBSD band contrast, typically yielding speeds of 500–800 EBSD patterns collected per second (50–80% of maximum). For instance, in order to collect a 3D EBSD dataset with well-defined subgrain orientation gradients, then the EBSD collection rate would likely need to be under 1500 pps. New methods such as dictionary indexing (DI) [63–67] and EMSphInx [68] are able to index EBSD patterns with relatively small resolutions (72 × 72 pixels), high noise, and low band contrast while maintaining angular orientation indexing resolution of 0.2–0.8° [69]. DI is substantially slower than Hough indexing however, currently limiting it to be an offline post-processing indexing mode, although the emerging EMSphInx method promises to increase the indexing speeds substantially [68].

The following actions may be incorporated into the workflow for a 3D experiment, depending on the data necessitated: femtosecond laser ablation and pole piece shutter insert/retract, glancing angle FIB milling (cleanup), stage movements, precision stage positioning by fiducial alignments with image processing scripts, detector insert/retracts (EBSD, EDS, BSE), EBSD data collection, EDS mapping, SE/BSE image collection, image processing for on-the-fly feature identification and FIB cleanup, automated electron beam tilt alignment and current measurements, and laser beam stability and power measurements. The example data collection times in Table 1 have been simplified to the primary detector imaging modes, laser ablation, FIB cleaning, and stage movements. More details about the TriBeam tomography setup can be found here [24].

3D datasets of nickel disk material were collected at different resolutions, as shown in Fig. 3, in order to characterize the γ' precipitates, high-resolution twin structure regions, and large volumes for grain and twin scale information. The resolution and sizes of the TriBeam datasets are summarized in Table 2.

A γ' precipitate dataset was collected from René 88DT using a FEI Quanta 3D DualBeam FIB-SEM with a ion beam sectioning resolution of 20 nm. A total volume of $5 \times 4.25 \times 4.5\,\mu m$ was reconstructed from 221 slices. BSE images from this dataset were segmented in the ImageJ/FIJI software package [70] and reconstructed to measure precipitate characteristics in this René 88DT polycrystalline superalloy.

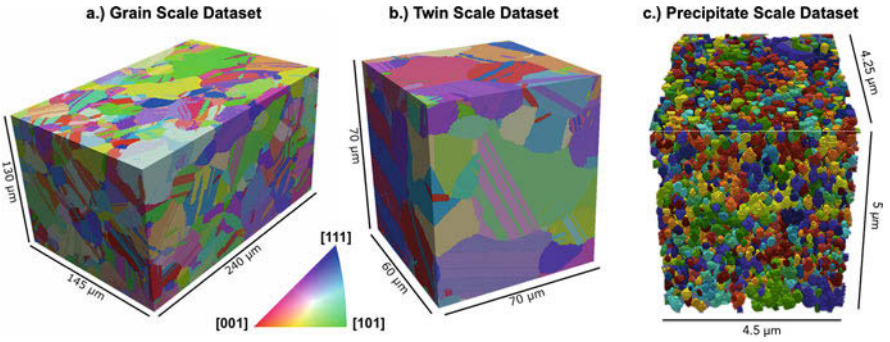

Fig. 3 TriBeam and FIB serial section datasets were collected from Ni-base disk material at resolutions to capture (left) large volumes of grain and twin data, (center) a high-resolution dataset containing detailed twin boundary regions, and (right) the γ' precipitates. The precipitate dataset coloring is showing individual precipitates as different random colors, whereas the grain and twin scale datasets are colored by IPF coloring

Table 2 Resolution, size, and dimensions of René 88DT 3D EBSD serial section datasets collected using the TriBeam microscope

Name	Resolution (µm)	Size (voxels)	Dimensions (µm)
Twin scale	$0.10 \times 0.10 \times 0.50$	$742 \times 993 \times 140$	$60 \times 70 \times 70$
Grain scale	$0.30 \times 0.30 \times 0.75$	$802 \times 482 \times 199$	$240 \times 145 \times 130$
Crack	$0.30 \times 0.30 \times 0.75$	$429 \times 757 \times 127$	$120 \times 200 \times 90$
Inclusion	$0.55 \times 0.55 \times 0.75$	$534 \times 802 \times 143$	$400 \times 600 \times 105$

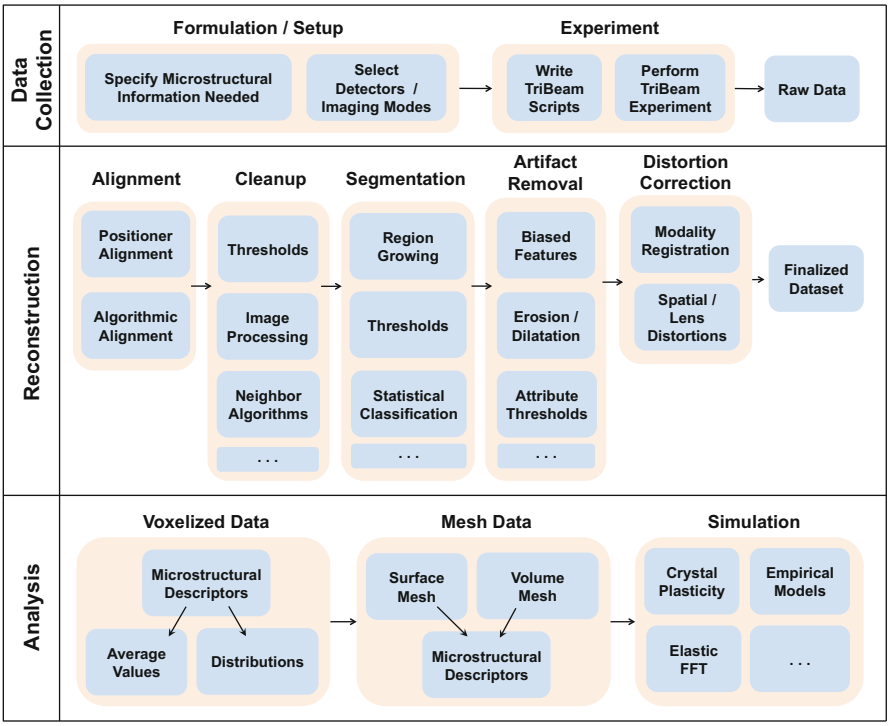

Fig. 4 The 3D EBSD data that is produced by the TriBeam requires a number of post-processing steps, which are described schematically here. Each dataset requires somewhat different parameters; however the core structure of that processing is relatively constant

A series of 3D EBSD TriBeam datasets were collected at various resolutions and at targeted features, including a fatigue crack initiation site and from a region where high-resolution digital image correlation (DIC) strain information had been collected [15, 71]. The characteristics of these René 88DT datasets are listed in Table 2, as well as an identifying name.

The workflow for acquiring, reconstructing, and analyzing 3D datasets is shown in Fig. 4. Briefly, this workflow includes defining data collection parameters that are closely tied to an understanding of the problem to be solved. These parameters include the 3D resolution necessary to capture the relevant microstructural features, which imaging modalities are required, or very specific parameters such as EBSD dwell time for pattern diffraction quality or potential pseudosymmetry complications [72–74]. Reconstruction of the 3D data happens next in the workflow, where a finalized dataset will be defined for analysis. Slice alignment, data cleanup, image segmentation, artifact removal, and distortion correction may be performed during this step. Data cleanup and artifact removal are always rooted in an understanding of the material via detailed 2D characterization. For instance, a minimum grain size filter may be applied if it is well-known that grains of a very small size do

not exist. Analysis of the data may be either based on voxelized or meshed data formats, depending on whether access to microstructural descriptors is desired, or direct property simulation. However, some microstructural descriptors may require meshed data formats as well, such as grain boundary inclinations.

For TriBeam EBSD datasets, DREAM.3D [75] is used to perform all reconstruction steps except for distortion corrections, which are performed using the methods described for strontium titanate [50] and a nickel superalloy [76]. The reconstruction steps can be clustered into four major groups: slice alignment, data cleanup, grain or feature segmentation, and artifact removal.

Although generating a preliminary dataset reconstruction is trivial with modern software tools, creating a high-quality reconstruction is still a significant challenge and often requires more time than dataset collection. Procedures that reduce noise or improve data quality greatly enhance the ability to extract high fidelity information from the dataset for modeling. Alignment and segmentation are by far the most difficult tasks. Alignment can be particularly challenging for small datasets where the morphology of a few dominant features dictates shifts computed during registration. Creating sample pedestals like the one fabricated using wire EDM shown in Fig. 5 that are small enough to collect data from the entire sample surface makes alignment significantly easier, and recovering the original sample shape provides a simple validation of alignment quality [20]. The pedestal fabrication procedure is a coarser scaled equivalency to the FIB procedures pioneered by Uchic. In many instances the pedestals used to collect data shown here were of the order of 1×1 mm in cross section by several mm in height. Orientation gradients and systemic misindexing due to pseudosymmetry are the most serious challenge for segmentation, when present.

Dataset volumes can become many terabytes in size, mostly due to the collection of raw EBSD patterns (EBSPs) or full spectrum EDS maps. The approximate scale

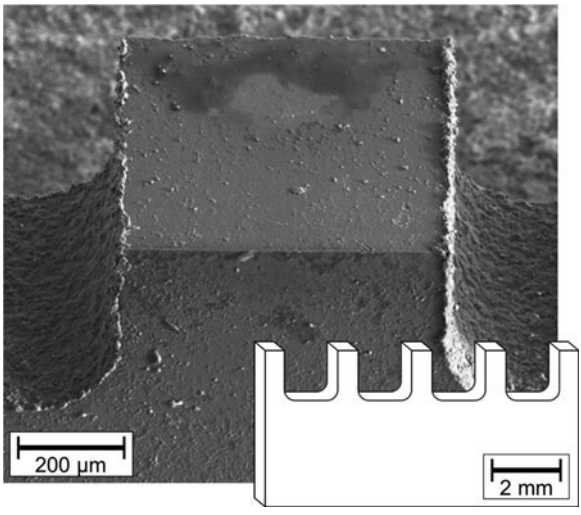

Fig. 5 Wire EDM is often used to create custom mm-scaled sample pedestals for targeted and untargeted TriBeam sectioning. The roughly 10 µm EDM heat-affected zone is mechanically polished away before TriBeam experiments or is located adjacent to a region where data will not be collected. The pedestal geometry is used in order to reduce material redeposition during laser ablation and to prevent shadowing of the EBSD signal at high sample tilt angles

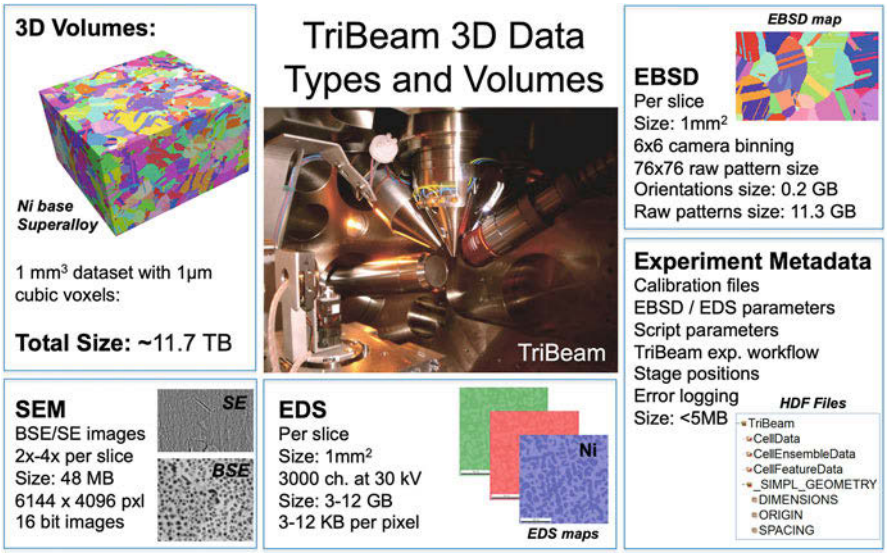

Fig. 6 Data usage is shown for the imaging modalities available during a hypothetical TriBeam experiment all scaled up for collection of 1 mm^3 of material at 1 µm cubic voxel size. Raw EBSPs, indexed EBSD maps, and EDS data take up the majority of the total data stored, with the rest being attributed to SEM images and metadata

of data usage is described in Fig. 6, where imaging data takes up much less than 1%, and the balance being EBSD indexed data, raw EBSPs, and full spectrum EDS data. EBSPs are stored so that re-indexing of the grain orientations can be performed with EMsoft dictionary indexing [63–66, 77], EMSphInx [68], or with higher-resolution Hough indexing parameters in the EDAX software OIM Analysis [78, 79]. EBSPs can scale to much larger sizes, depending on the EBSD detector resolution and whether a binning mode is used. For instance, using a EDAX Hikari camera to capture EBSPs at each mapping location can generate patterns of size 76×76 pixels for $6\times$ binning (as shown in the example in Fig. 6) up to full resolution patterns of roughly 480×480 pixels. Full spectrum EDS mapping also can require massive amounts of data storage, with 1000 channels typically recorded per 10 kV electron beam energy. Depending on the data type chosen to store the arrays and assuming 30 kV electron accelerating voltage, 3–12 KB is consumed for each spectrum, resulting in 3–12 GB per mm^2 mapping area at 1 µm resolution. The challenges with gathering such large full spectrum EDS data and detailed analysis are described in more detail elsewhere [80]. During an experiment, metadata such as the detector configurations and calibrations, stage position logs, hardware error logging (microscope, femtosecond laser and output, optics beamline, EBSD, EDS), and script parameters are all stored in HDF5 data containers similar to those formulated by Jackson and De Graef [81].

4 Targeted 3D Data

The microstructural configuration (neighborhood) is demonstrated to be influential to the initiation of fatigue cracks [6, 7, 9, 82]. A postmortem analysis of fatigue samples is a good way to identify systematic microstructural characteristics that result in fatigue cracks. Samples of René 88DT were cycled with fully reversed loading and then interrupted at 80% lifetime (R = −1, 1 Hz, peak load 758 MPa) such that the regions surrounding the initiated fatigue cracks could be investigated. Previous work has shown that this polycrystalline superalloy spends much of its life (80%) initiating cracks [82], before they propagate into the next few grains and then begin short crack-type growth.

A dataset was gathered in the TriBeam system from a region where a typical fatigue crack had initiated. The FIB was used to clean a 250-μm-wide region after femtosecond laser ablation using a 15 nA, 30 kV Ga^+ beam at an angle of 3° to the surface. Although EBSD maps containing high-quality diffraction patterns are obtainable from the laser-ablated surface in René 88DT, FIB cleaning was still performed in order to guarantee that small and thin twin features (<1 μm) were well resolved. The total collection time per slice was 53 min, with 28 min EBSD collection, 20 min FIB, and the balance stage movements and SEM imaging. The dataset is comprised of 127 slices collected at a 0.75 μm slice thickness and 0.3 μm EBSD resolution.

Both the 3D fatigue crack location and the microstructural neighborhood at the surface and subsurface were reconstructed. Twin boundaries are visible adjacent to the crack initiation location in Fig. 7, as expected based on the room temperature

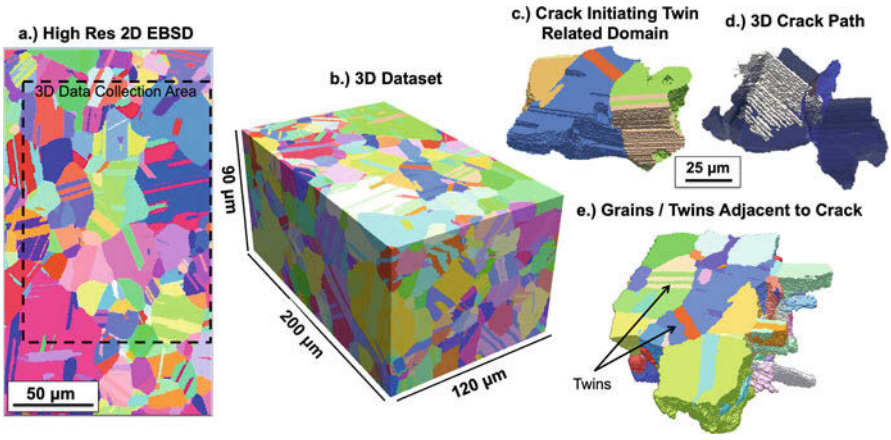

Fig. 7 A region containing a crack (**a**) was identified and a targeted 3D dataset collected beneath (**b**) in order to investigate the microstructure and local loading conditions leading to failure. The 3D dataset is 200 × 120 × 90 μm with a 0.75 μm slice thickness and 0.3 μm EBSD resolution. The crack initiating twin related domain (**c**) and the crack path (**d**) are shown along with the microstructure surrounding the crack path (**e**)

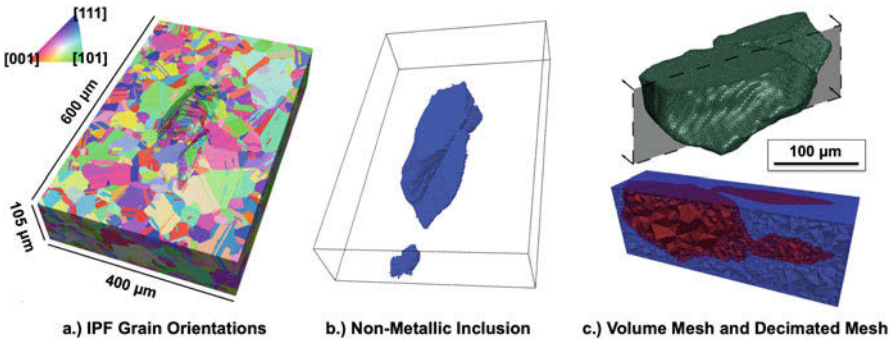

Fig. 8 (Left) reconstruction of a targeted TriBeam dataset containing the grain structure surrounding a nonmetallic inclusion (center) and a volume mesh of the inclusion for use in finite element modeling (right)

fatigue crack initiation criterion developed previously for polycrystalline superalloys [9, 82]. Briefly, this criterion predicts crack initiation in highly loaded grains (large Schmid factor) where the slip trace is parallel to a large twin boundary, and the elastic mismatch between the twin and parent grain are large.

Nonmetallic inclusions have been shown to initiate cracks in polycrystalline nickel superalloys, particularly at elevated temperatures (400–650 °C) during high cycle fatigue at stresses near 768–965 MPa [6, 7]. The crystallographic configuration surrounding an inclusion, particularly in the vicinity of peak stress concentrations, is of particular importance to the localization of strain and eventually the initiation of cracks [6, 7, 13, 14, 83]. A targeted 3D dataset was collected for a volume containing a crack initiating nonmetallic inclusion, shown in Fig. 8. The inclusion was volume meshed according to the details in [84], and mechanical loading was simulated using Abaqus. Direct comparisons between the simulation and DIC strain measurements showed good qualitative agreement, particularly when the interface between the matrix and inclusion is considered to be debonded [83]. The DIC measurements capture the localization of strain into bands along twin boundaries, whereas the elastic regime Abaqus simulations show a continuum representation. The exact details of this comparison can be found elsewhere [83, 84].

While not discussed here, the third phase of the workflow is analysis of the 3D dataset. This often requires development of algorithms and specialized routines to extract information from the dataset. Given the size of these datasets, it should be emphasized that manual analysis of features is rarely feasible. In addition to traditional stereological measurements, 3D data enables calculations not possible in 2D. Some unique 3D measurements are well established but nontrivial, e.g., degree of coherence of the twins in these René 88DT datasets requiring careful surface meshing to measure boundary normals [9, 84]. Significant capacity for novel analyses also exists, e.g., characterizing twin related domains via connectivity networks.

5 Future Needs

The most obvious limitation of the TriBeam approach, like most other 3D techniques, is the cost and time required for acquisition and reconstruction of the dataset. Crystallographic orientation mapping in SEM is usually performed via EBSD, which has seen recent speed improvements with the replacement of CCDs with CMOS cameras into standard phosphor-optics-type setups. It is likely that rates will continue somewhat with direct electron (DE) detectors, which may also have the advantage of enhanced electron sensitivity. We expect these CMOS and DE systems combined with emerging indexing algorithms [63–66, 68, 77] will decrease collection times and increase data mapping quality. The other significant time restriction is (if necessary) the glancing angle surface cleaning of the femtosecond laser-ablated surfaces. Currently the TriBeam uses a Ga^+ FIB with 65 nA beam current. Xenon plasma FIBs are available and have been integrated into a new prototype TriBeam [60] to produce currents up to 20 times higher than a Ga^+ FIB [85], which can scale to a similar 20× surface cleanup rate increase, depending on the material.

Data sharing, provenance, and portability have become a key issue for the large-scale and collaborative efforts required to tackle scientific problems with 3D data. A new software and data infrastructure, BisQue [86–88], has been useful for addressing the data challenges and providing a platform on which data versions can be synchronized between collaborative institutions and parallelized, parameterized processing of data workflows is possible.

Data merging from various modalities including HR-DIC, synchrotron X-ray DCT, and TriBeam tomography is challenging due to the complex distortions associated with each experimental method. For instance, SEMs can have spatial distortions and drift distortions from the electron optics and sample charging effects [71, 89]. New algorithms are being developed to perform and address data merging including those used for combining synchrotron diffraction contrast tomography and TriBeam tomography [50] and a generalized multimodal data merging approach using an evolutionary optimization machine learning algorithm [76].

Furthermore, developments in digital image correlation (DIC) via high-resolution DIC and Heaviside-DIC [90] and coupling with EBSD data are being used to predict strain localization, slip transmission across boundaries, and how strain can create “microvolumes” [91], where non-Schmid-type loading conditions are imposed on adjacent grains across a grain boundary. Opportunities for the targeted investigation of the influence of the subsurface 3D grain structure on strain localization and transmission phenomenon are also emerging.

At the precipitate scale, the glide of dislocations that locally shear precipitates results in strain localization along twin boundaries [15, 16, 71, 92, 93]. These are ultimately sites for crack initiation, and their intersection with grain boundaries dominates the early stages of crack growth [6, 12, 94–98]. The new 3D characterization capabilities described here, in combination with multiscale plasticity models, ultimately enable much higher fidelity prediction of properties such as yield strength